

PHYSICAL REVIEW LETTERS

VOLUME 60

16 MAY 1988

NUMBER 20

Long-Time Tails in a Chaotic System

Koo-Chul Lee

Department of Physics, Seoul National University, Seoul 151, Korea

(Received 16 February 1988)

The long-time tail in the diffusive behavior in a strongly chaotic system (stadium billiard) is studied from the point of view of “stickiness” of invariant lines. Diffusion near the invariant line in the phase space can be described by a one-dimensional continuous random-walk problem with pausing time which is inversely proportional to the distance from the line. The problem is studied by numerical methods and it is shown that the first-passage-time distribution has an algebraic decay tail in the form $\sim t^{-\nu}$ with the estimated exponent $\nu = 2.933 \pm 0.005$.

PACS numbers: 05.60.+w, 05.45.+b

It is generally believed that the origin of long-time correlations in chaotic dynamical systems is due to the effects of integrable components in the chaotic region. For the purpose of studying the effects of integrable components in the chaotic region, either analytically or numerically, two-dimensional area-preserving maps are often used as a model for simple Hamiltonian systems.¹⁻⁵ Integrable components in these models are invariant lines constituting the border of the chaotic region or boundary circles⁶ of islands in the chaotic region.

The long-time correlation effects of these lines usually appear as “stickiness” of these lines. When an orbit is once trapped close to the invariant lines, it stays stuck for a long time before it returns to the chaotic sea. The slow diffusion near the integrable region is often characterized by the long-time tail of an algebraic decay in either the survival probability or its time derivative, the first-passage-time distribution. Recently I made detailed analysis of the origin of the stickiness of the invariant line of a certain model dynamical system⁷ slightly perturbed from the integrable one. A similar analysis can be made of the stadium problem,⁸ although the existence of the integrable component near the invariant line in this problem is intuitively obvious, in contrast to the case of the abstract model dynamical system where the dynamical behavior near the invariant line is not easy to analyze. In general, the location of the invariant line itself is hard to predict in perturbed dynamical systems,

let alone the dynamical behavior in the vicinity of the line. Therefore the lesson we learn from the stadium problem can give an insight to the chaos problem in the abstract dynamical system where chaos is generated from a small nonintegrable perturbation. On the other hand, we can gain some more understanding on the nature of chaos in the stadium problem or similar dynamical systems such as the convergent hyperbolic orbits, existence of homoclinic orbits, horseshoe map, etc., besides the general mathematical results already known. In this sense the comparative study of two dynamical systems can enrich our understanding of the chaotic behavior of dynamical systems in general.

Let us consider a billiard model in the stadium (Fig. 1), which is known to belong to a class of B systems, and hence is a K system.⁸ Noting that near the invariant line of period 2 there are integrable components of arbitrarily long length in the time evolution of chaotic orbits, Vivaldi, Casati, and Guarneri⁹ calculated the velocity autocorrelation function by taking the phase average instead of the time average since the orbit is ergodic. They found that the velocity autocorrelation function has an algebraic decay tail with its exponent 3.

In this Letter I will follow a somewhat different route to show that the integrable component slows down the diffusion near the invariant line. The motion of a billiard elastically reflecting from the stadium-shaped boundary as in Fig. 1 can be conveniently described by an area-

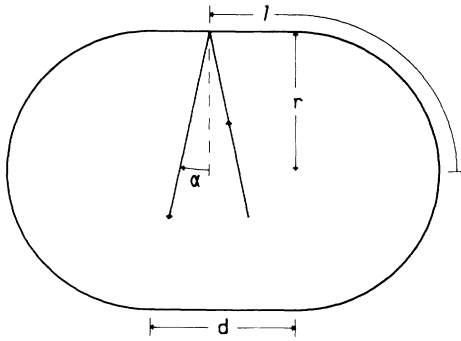


FIG. 1. Stadium.

preserving mapping by the introduction of the so-called Birkhoff coordinates.⁹ These coordinates consist of a pair of real numbers that specify, for each collision with a boundary, the point of impact l and the tangent component (with respect to the boundary) $s = |\mathbf{v}| \sin \alpha$ of the velocity \mathbf{v} at the point l right after the collision, where α is the angle of reflection. Since a pair (l, s) uniquely determines the pair (l', s') of the next collision, we can define a mapping T by $(l', s') = T(l, s)$. It can be shown that T preserves the area.

The boundary of the stadium consists of four components of curves, namely, two straight side lines (zero curvature or neutral) of length d and two semicircles (negative curvature or focusing) of radius r in the end zones. If we take the origin of variables l at the midpoint of the right-hand semicircle (Fig. 1), and take $|\mathbf{v}| = 1$, $d = (1 + \pi\rho)^{-1}$, and $r = \rho d$, then we can restrict the phase space of the system to the square $[-1, 1] \times [-1, 1]$, where ρ is the parameter representing the ratio r/d . There are two types of invariant lines in this phase space, namely, the lines $s = \pm 1$ and $|l| = [\pi r/2, d + \pi r/2]$ on the line $s = 0$. The first type corresponds to the billiard motion which rolls along the boundary of the stadium and the second type corresponds to the billiard motion bouncing between two side lines perpendicularly. The dynamical behavior in the vicinity of these invariant lines shows stickiness of the line, a typical characteristic of phase behavior near the invariant line.

Although the period of convergent periodic orbits⁷ diverges as the orbits approach both invariant lines, only invariant lines of the second type contribute to the long-time tail since the time between successive collisions on the semicircles in the limit of the rolling motion along the arc approaches zero in the case of the first type. For this reason I will restrict the discussion to the invariant line of the second type and hereafter only the second kind is implied when I mention the invariant line. A typical orbit in the phase space is shown in Fig. 2.

When a phase point moves near the invariant line the distance s from the line is conserved. Every iteration of T^2 moves the point a distance $\Delta l = 4r|s|/(1-s^2)^{1/2}$ parallel to the line. When the point comes near the end

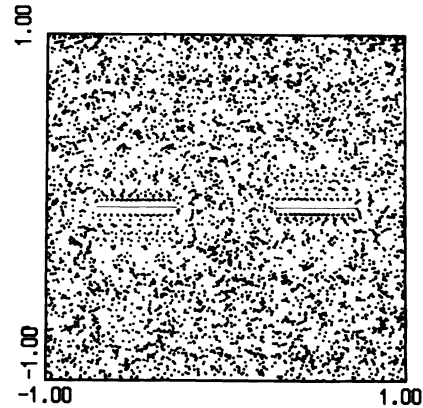


FIG. 2. A typical phase-space orbit with $\rho = 0.4$, $s_l = \sqrt{3} - 1$, $l_l = \sqrt{2} - 1$, and 5000 iterations. The two straight lines in the center of the "button holes" are the period-2 invariant lines. Stickiness of the line is "negatively" manifested by the orbit, since the orbit is ergodic.

of the side line (which will be called the end point with its l value denoted by l_e), it enters the region of a semicircle and after either single or double collisions on the wall of semicircle it is reflected back to side lines if the incident angle $\alpha = \sin^{-1}s$ is sufficiently small. Therefore one can say that the orbit near the invariant line is made of regular components of constant s and transitions between them.

Let us examine the law of transition in further detail. Although the transition starts when the phase point comes to a point less than Δl short of the end point, it is sufficient to consider only points within the distance $\Delta l/2$ from the end point since if it is farther away than $\Delta l/2$ it will not enter the region of the semicircle but be reflected to the opposite side line. Although it is a straightforward matter to obtain the law of transition I will not present the general expression since it is not only too complex to present but also irrelevant to the long-time behavior of this dynamical system. Instead, I will describe general characteristics of the transition and the behavior in the limit of small s which is relevant to the long-time behavior. It is convenient to describe the new angle $\alpha' = \sin^{-1}s'$ in terms of the old angle $\alpha = \sin^{-1}s$ and the fractional distance, $\lambda = |l - l_e|/(\Delta l/2)$ of the old l .

Let

$$\lambda_0 = \frac{\sin 2\alpha / \sin \alpha + \cos 2\alpha + 1}{2(\sin 2\alpha / \sin \alpha + \cos 2\alpha)},$$

which takes a value in the interval $(0.5, 0.75)$. When λ varies from 0 to λ_0 , α' decreases monotonically from 3α to $\alpha/3$ passing the value α at $\lambda = 0.5$. When λ varies from λ_0 to 1, α' increases monotonically from $\alpha/3$ to 3α passing the value α at $\lambda = 0.75$ (Fig. 3). When $\lambda \in [0, \lambda_0]$, the billiard comes out to the same side line after a single reflection against the semicircle, while when $\lambda \in [\lambda_0, 1]$, it comes out to the opposite sideline,

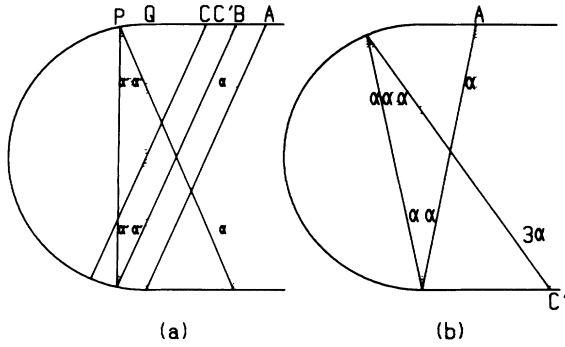


FIG. 3. (a) The geometrical construction to show the rule of reflection near the end point. Here $QA = \Delta l/2$, $QC/QA = 0.5$, $QC'/QA = \lambda_0$, and $QB/QA = 0.75$. (b) The full orbit starting at A is redrawn and the orbit starting at C' can be visualized from the inverted picture. The orbit starting at Q can also be constructed from the part of inverted picture of (b).

after double reflection as we can see from Fig. 3.

For small α , λ_0 can be approximated by $\lambda_0 \approx \frac{2}{3} = 0.666\dots$. In Fig. 4 I plot the line segment of length $\Delta l/2$ starting at $l = l_e - 5\Delta l/6$ on $s = 10^{-3}$ and its T^3 image on the same phase region by reversing the sign of l' , i.e., $l' \rightarrow -l'$. This was done by my noting that when l is farther away than $\Delta l/2$ and within the distance $5\Delta l/6$ from the end point, the billiard moves to the opposite side line and within the distance $\Delta l/3$ from the end point by a single reflection so that it returns to the same side line after one more reflection from the semicircle.

When the billiard takes a new s value it stays roughly for a time

$$\tau = \text{Int}[1/(2s\rho)] + 1, \tag{1}$$

since if s is sufficiently small, the time it takes to move from one end point to the other is approximately $d/2rs$ in units of a single collision time. In (1) $\text{Int}(x)$ is the integer part of x and 1 is added to account for the time it takes to make the transition from old s to new s' . From Fig. 4 it is clear that the transition probability W from old s to new s' is uniform over the interval $(s/3, 3s)$, i.e.,

$$W(s',s) = 3[\theta(s' - s/3) - \theta(s' - 3s)]/8s \tag{2}$$

with normalization. In the above $\theta(s)$ is the step function defined as

$$\theta(s) = \begin{cases} 1, & s \geq 0 \\ 0, & s < 0. \end{cases}$$

We can view this problem as a continuous random walk with pausing time given by (1). In our previous example,⁷ we had $(s/2, 2s)$ instead of $(s/3, 3s)$ for the range that the walker takes in a single step.

We can now trace the origin of the random transition from the randomness of the initial condition since we can see from Fig. 4 that every time the transition from s to s'

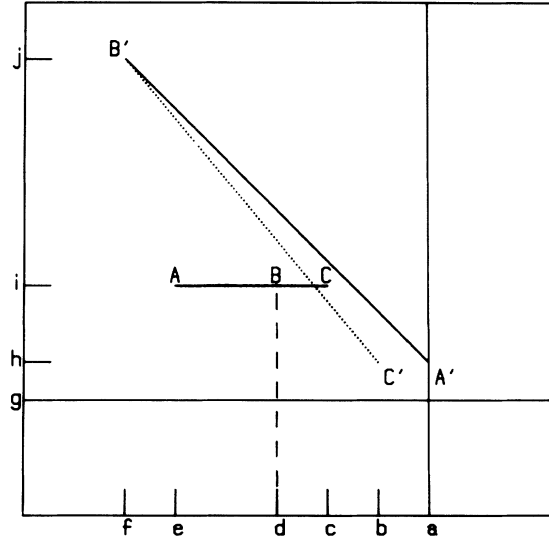


FIG. 4. $A'B'C'$ is the T^3 image of line segment ABC (with $l' \rightarrow -l'$) made of 300 points with each primed position corresponding to the image of an unprimed position. a represents the end point l_e and g indicates the $s=0$ line where the invariant line is located. In this picture $\rho = \frac{8}{3}$ and $ig = s = 10^{-3}$. If s is small as in this picture $ab=bc=cd=ef=AC/3$ and $ig=3hg=jg/3$.

is made, finer specification of the initial values of the orbit is amplified (as the line segment ABC is stretched to $A'B'C'$) and determines the next transition.

I have solved this random-walk problem by Monte Carlo method. I place N_0 particles at a certain position s_0 and let them execute a random walk by the rules (1) and (2) and record the time they take to pass an arbitrarily set boundary point s_b for the first time. For the purpose of comparison with the result of Ref. 7 I chose $\rho = \frac{4}{3}$ to make the pausing time (1) exactly the same and $s_0 = 0.005$ and $s_b = 0.15$ to make the setting for the Monte Carlo simulation exactly the same as in Ref. 7. Figure 5 is a log-log plot of the number of particles $N(t)$ versus the first passage time (in units of 64 collisions). They clearly indicate that the first-passage-time distribution $P_{\text{fpt}} = N(t)/N_0$ has an asymptotic algebraic decaying tail in the form of

$$P_{\text{fpt}} \propto t^{-\nu}. \tag{3}$$

When we estimate the slope and standard deviation from the data by the χ^2 -fit method we obtain

$$\nu = 2.933 \pm 0.005. \tag{4}$$

The straight line of the χ^2 fit is drawn in Fig. 5. The value (4) is somewhat larger than 2.80 ± 0.01 in Ref. 7 presumably because of faster diffusion (wider range per random-walk step) given by (2).

In closing I would like to point out that the fact that we find exactly the same diffusive characteristics in the

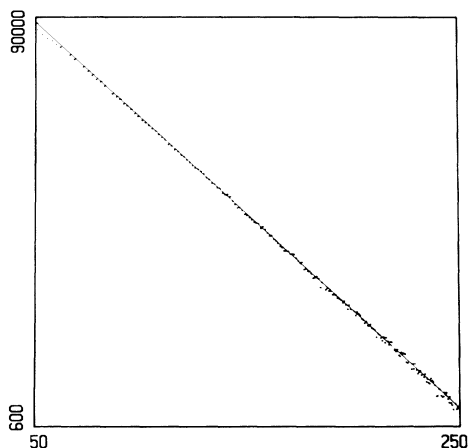


FIG. 5. Log-log plot of the first-passage-time distribution. The ordinate is the number and the abscissa is the time in units of 64 collisions.

two apparently quite different dynamical systems, the present problem and the one in Ref. 7, is suggestive that the behavior shown in these examples is generic diffusive

behavior near the invariant line.

I wish to thank Professor D. Kim and Professor M. Y. Choi for their critical reading of the manuscript and valuable suggestions. This work was supported in part by the Korea Science and Engineering Foundation research grant.

¹S. R. Channon and J. L. Lebowitz, *Ann. N.Y. Acad. Sci.* **357**, 108 (1980).

²B. V. Chirikov and D. L. Shepelyanski, *Physica (Amsterdam)* **13D**, 394 (1984).

³C. F. Karney, *Physica (Amsterdam)* **8D**, 360 (1983).

⁴R. S. Mackay, J. D. Meiss, and I. C. Percival, *Physica (Amsterdam)* **13D**, 55 (1984).

⁵J. D. Meiss and E. Ott, *Phys. Rev. Lett.* **55**, 2741 (1985).

⁶J. M. Greene, R. S. Mackay, and J. Stark, *Physica (Amsterdam)* **21D**, 267 (1986).

⁷K. C. Lee, "What Makes Chaos Border Sticky?" (to be published).

⁸L. A. Bunimovich, *Commun. Math. Phys.* **65**, 295 (1979).

⁹F. Vivaldi, G. Casati, and I. Guarneri, *Phys. Rev. Lett.* **51**, 727 (1983).